Optimized Runge–Kutta (LDDRK) schemes with non-constant-amplitude waves

Aldaïr Petronilia* and Edward James Brambley†
University of Warwick, Coventry CV4 7AL, United Kingdom

Optimized finite differences (a.k.a. DRP schemes) and optimized Runge–Kutta time stepping (e.g. LDDRK schemes) are commonly used in Computational AeroAcoustics simulations to accurately represent waves with the least computational cost. Recently, it was suggested that optimized DRP spatial derivatives perform poorly for growing and decaying waves, as their optimization implicitly assumes real wavenumbers. Here, the comparable question of the performance of optimized Runge–Kutta time stepping schemes for non-constant-amplitude waves is considered. Not only is it found that optimized Runge–Kutta schemes perform more poorly than their maximal order equivalents for non-constant-amplitude waves, it is also found that significantly more accuracy for the same computation cost can be achieved by replacing an alternating scheme such as LDDRK56 with a single Runge–Kutta scheme with a longer time step (such as an 11-stage Runge–Kutta scheme with twice as long a time step). These theoretical predictions are demonstrated in practice using a realistic 1D wave-propagation example.

I. Introduction

Computational AeroAcoustics (CAA) simulations are an important tool in investigating aircraft noise in realistic geometries and flows. Unlike Computational Fluid Dynamics (CFD) simulations, CAA simulations are designed to accurately propagate small amplitude oscillations over the entire computational domain, and are therefore poised on a knife edge between being overly dissipative on the one hand and being unstable on the other. Finite difference schemes to calculate spatial derivatives, and Runge–Kutta and Adams–Bashforth schemes to step forwards in time, have all been optimized to attempt to accurately propagate acoustic perturbations with few points per wavelength and steps per period respectively, and such schemes are commonly used in modern CAA simulations. Examples of optimized spatial derivatives include: the by-now classic 7-point 4th order explicit DRP schemes [1, 2]; optimized implicit/compact schemes of up to 6th order [3, 4]; prefactored implicit MacCormack schemes [5]; trigonometrically optimized schemes [6]; 2nd and 4th order 9, 11, and 13 point schemes [7]; and asymmetric optimized schemes for use near boundaries [8, 9]. Examples of optimized timestepping schemes include: an optimized Adams–Bashforth scheme [1]; Low Dispersion and Dissipation Runge–Kutta (LDDRK) 5-step, 6-step and alternating 4/6- and 5/6-step schemes [10]; and optimized 5- and 6-step Runge–Kutta schemes [7]. Rona et al. [11] even considered jointly optimizing spatial derivatives and time stepping schemes to give the best wave propagation properties when combined, although this analysis is dependent on the dispersion relation of the system being simulated, while the previously mentioned schemes are applicable to general dispersion relations..

Most of the optimized spatial and time-stepping schemes investigate the action of the scheme in the wavenumber/frequency domain. For example, the solution to the time-stepping problem $\mathrm{d}\boldsymbol{U}/\mathrm{d}t = \boldsymbol{F}(\boldsymbol{U}, t)$ for the p-stage low-storage Runge–Kutta scheme considered by Hu, Hussaini, and Manthey [10] is

$$\boldsymbol{U}(t+\Delta t) = \boldsymbol{U}(t) + \beta_p \boldsymbol{K_p}, \qquad \text{where} \qquad \boldsymbol{K_{j+1}} = \Delta t \boldsymbol{F}\big(\boldsymbol{U}(t) + \beta_j \boldsymbol{K}_j,\, t + \beta_j \Delta t\big), \tag{1}$$

with $\beta_0 = 0$. Assuming $F(\boldsymbol{U}, t)$ to be linear in $\boldsymbol{U}$ and time invariant, and transforming to the frequency domain (or equivalently considering $F(\boldsymbol{U}, t) = -\mathrm{i}\omega\boldsymbol{U}$), this scheme results in

$$\boldsymbol{U}(t+\Delta t) = r(\omega\Delta t)\boldsymbol{U}(t), \qquad \text{where} \qquad r(\omega\Delta t) = 1 + \sum_{j=1}^{p} c_j(-\mathrm{i}\omega\Delta t)^j \qquad \text{and} \qquad \beta_{p-j} = c_{j+1}/c_j \tag{2}$$

with coefficient $c_1 = \beta_p$. The exact solution would have $\boldsymbol{U}(t+\Delta t) = \boldsymbol{U}(t) r_e(\omega\Delta t)$ with $r_e(\omega\Delta t) = \exp\{-\mathrm{i}\omega\Delta t\}$, while the numerics instead gives $\boldsymbol{U}(t+\Delta t) = \boldsymbol{U}(t) r(\omega\Delta t)$ with $r(\omega\Delta t) = \boldsymbol{U}(t)\exp\{-\mathrm{i}\bar{\omega}\Delta t\}$. One could choose the coefficients

*Undergraduate, University of Warwick
†Associate Professor, University of Warwick, AIAA senior member.

$c_j = 1/j!$ so that $|r(\omega\Delta t) - r_e(\omega\Delta t)| = O\big((\Delta t)^{p+1}\big)$ in the limit $\Delta t \to 0$; this is referred to as a pth-order accurate scheme, and since it is the best that can be achieved with a p-stage Runge–Kutta scheme, we refer to such schemes here as maximal order. In contrast, one could instead vary the coefficients c_j in order to minimize an error of the form

$$e = \int_0^\eta |r(\omega\Delta t) - r_e(\omega\Delta t)|^2 \,\mathrm{d}(\omega\Delta t), \qquad \text{or} \qquad E = \int_0^\eta |\bar{\omega}\Delta t - \omega\Delta t|^2 \,\mathrm{d}(\omega\Delta t), \tag{3}$$

subject to constraints of a minimum order of accuracy (typically 2nd or 4th order accuracy as $\Delta t \to 0$) and stability (meaning $|r| \leq 1$ for $0 \leq \omega\Delta t < \eta_s$). Optimization of e was performed by Hu et al. [10], while Tam and Webb [1] optimized the equivalent of E for an Adams–Bashforth scheme*. A similar optimization method may be performed for spatial derivative schemes in terms of the spatial wavenumber $k\Delta x$ instead of the frequency $\omega\Delta t$ [see, for example, 1].

Recently [12], it was suggested for spatial derivatives that optimization of a metric such as (3) which assumes real $k\Delta x$ results in a scheme which performs well for constant amplitude waves corresponding to real k, but which performs poorly for waves of non-constant amplitude corresponding to complex k. Unfortunately, non-constant amplitude waves are rather common in aeroacoustics, especially in the vicinity of acoustic linings, for high-order spinning modes which decay rapidly away from duct walls, close to near-singularities such as sharp trailing edges or strongly localized sources, and for instabilities. Attempts at reoptimizing spatial derivatives to perform well for both non-constant and constant amplitude waves [13] concluded that, with sufficient a priori knowledge of expected wavenumbers, optimized derivative schemes could be constructed to perform well, but that in general, and certainly for broadband excitation, maximal order schemes were more likely to be more accurate.

The purpose of this paper is to investigate the comparable situation for timestepping schemes. In particular, we consider how well common schemes (such as the LDDRK56 scheme [10]) which are optimized using metrics such as (3) perform when $\omega\Delta t$ is not real, corresponding to waves which decay or grow exponentially in time.

II. Theoretical comparison of Runge–Kutta time stepping schemes

Any Runge–Kutta scheme solves the differential equation $\mathrm{d}\boldsymbol{U}/\mathrm{d}t = -\mathrm{i}\omega\boldsymbol{U}$ to give $\boldsymbol{U}(t + \Delta t) = \boldsymbol{U}(t)r(\omega\Delta t)$, where $r(\omega\Delta t)$ is given by (2) with some constants c_j. We define the phase error of such a scheme by

$$\varepsilon_p = \left|\frac{\bar{\omega} - \omega}{\omega}\right| = \left|\frac{\bar{\omega}}{\omega} - 1\right|, \qquad \text{where} \qquad \bar{\omega}\Delta t = \mathrm{i}\log\big(r(\omega\Delta t)\big), \tag{4}$$

and the branch of the logarithm is chosen so that $|\bar{\omega}\Delta t - \omega\Delta t|$ is minimized. Similarly, we define the group velocity error

$$\varepsilon_g = \left|\frac{\mathrm{d}\bar{\omega}}{\mathrm{d}\omega} - 1\right|. \tag{5}$$

Finally, we define the amplification factor error

$$\varepsilon_r = \left|\frac{r(\omega\Delta t) - r_e(\omega\Delta t)}{r_e(\omega\Delta t)}\right| = \big|r(\omega\Delta t)\exp\{\mathrm{i}\omega\Delta t\} - 1\big|. \tag{6}$$

Assuming these errors are small, the relative global error for a simulation up to time $t = T$ compared with the exact solution $\boldsymbol{U_e}(t)$ is then given by

$$\frac{\|\boldsymbol{U}(t) - \boldsymbol{U_e}(t)\|}{\|\boldsymbol{U_e}(t)\|} = \left|\frac{r(\omega\Delta t)^{T/\Delta t} - r_e(\omega\Delta t)^{T/\Delta t}}{r_e(\omega\Delta t)^{T/\Delta t}}\right| \approx \frac{T}{\Delta t}\varepsilon_r \approx T\omega\varepsilon_p. \tag{7}$$

A. Phase errors for complex frequencies

We first consider the non-alternating Low Dispersion and Dissipation Runge–Kutta (LDDRK) schemes of Hu et al. [10]. Figure 1 compares the phase error ε_p of these optimized LDDRK schemes with their maximal order Runge–Kutta equivalents with the same number of steps, and hence with the same computational expense. As expected, the optimized schemes perform better along the real $\omega\Delta t$ axis, at the expense of their behaviour near the origin and for non-real $\omega\Delta t$. In order to better compare the schemes, it is helpful to plot which is more accurate for any given value of $\omega\Delta t$. Figure 2 compares the maximal order and LDDRK [10] optimized schemes for 4, 5 and 6 stages. The green

*Note that Tam and Webb [1] used the opposite notation to that used here, in that they used $(\bar{\omega}, \omega)$ where here we use $(\omega, \bar{\omega})$.

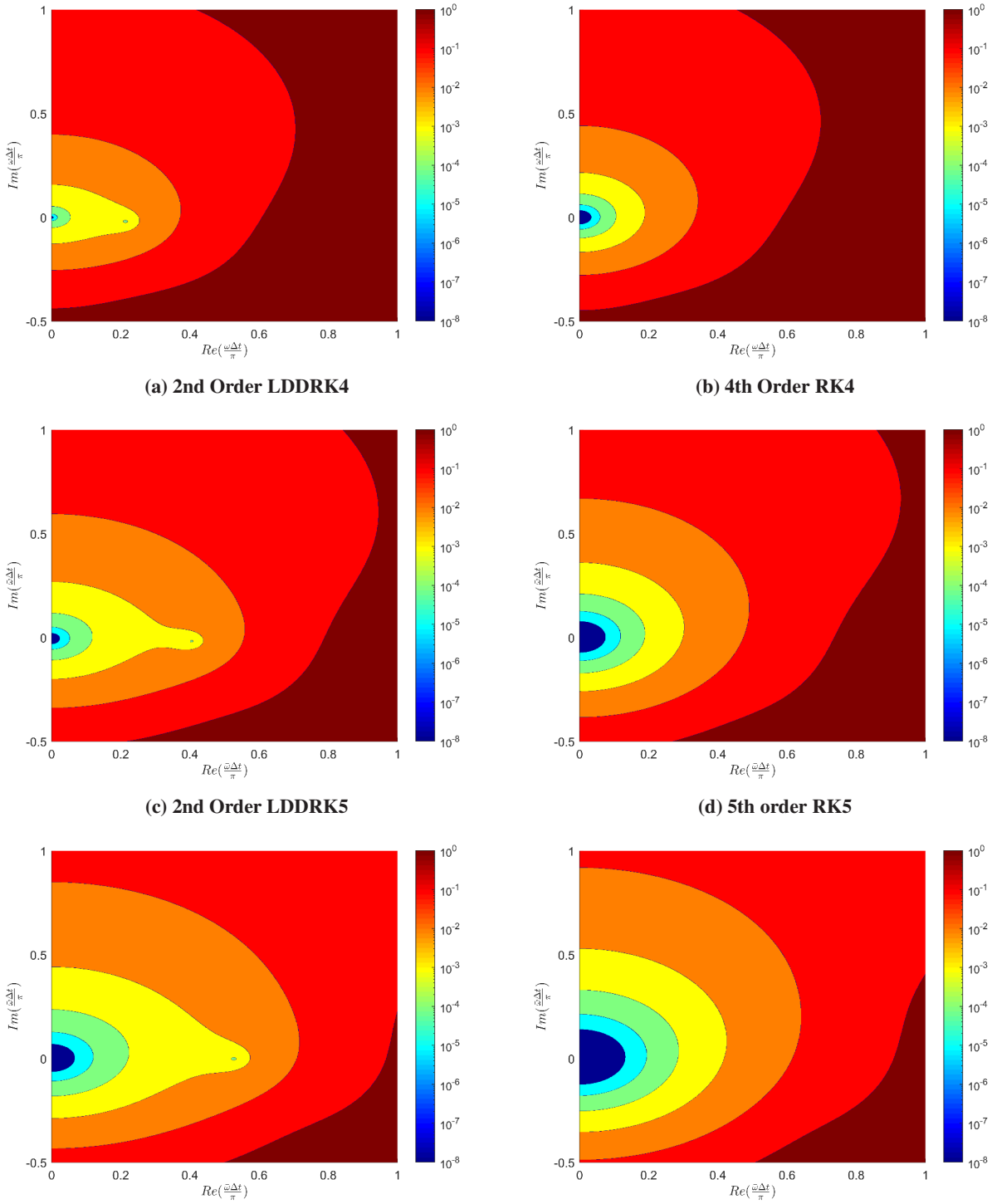

(a) 2nd Order LDDRK4 **(b) 4th Order RK4**

(c) 2nd Order LDDRK5 **(d) 5th order RK5**

(e) 4th order LDDRK6 **(f) 6th order RK6**

Fig. 1 Plots of phase error ε_p in the complex $\omega\Delta t$ plane for 4, 5 and 6-stage Runge-Kutta schemes. (a) and (b) are 4-stage, (c) and (d) are 5-stage, and (e) and (f) are 6-stage. (a) and (c) are optimised 2nd order schemes [10], (e) is an optimized 4th order scheme [10], while (b), (d), and (f) are maximal order schemes.

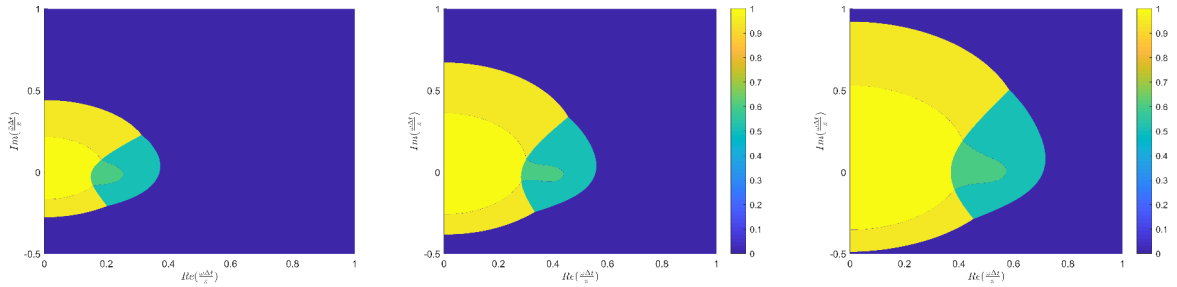

(a) 4th Order vs LDDRK4 **(b) 5th Order vs LDDRK5** **(c) 6th Order vs LDDRK6**

Fig. 2 Comparison in the complex $\omega\Delta t$ plane of where the maximal-order (yellow) or LDDRK (green) schemes are more accurate for the 4, 5 and 6 stage schemes. Darker regions indicate where neither scheme is 0.1% accurate ($\varepsilon_p > 10^{-3}$), while violet regions indicate where neither scheme is 1% accuracy ($\varepsilon_p > 10^{-2}$).

regions show where the LDDRK optimized schemes outperform the maximal order schemes, but operating within such a region would need significant a priori knowledge of the calculation to be performed, and remaining in this region would be nearly impossible for broadband simulations.

Hu et al. [10] further proposed two two-stage alternating schemes. For a p_1-p_2 scheme, the first timestep uses a p_1-stage Runge-Kutta scheme and the second timestep uses a p_2-stage Runge-Kutta scheme. This results in $\boldsymbol{U}(t+2\Delta t) = \boldsymbol{U}(t) r_1(\omega\Delta t) r_2(\omega\Delta t)$, where the amplification factors of the first and second steps are

$$r_1(\omega\Delta t) = 1 + \sum_{j=1}^{p_1} a_j (-\mathrm{i}\omega\Delta t)^j = \mathrm{e}^{-\mathrm{i}\bar{\omega}_1\Delta t}, \qquad r_2(\omega\Delta t) = 1 + \sum_{j=1}^{p_2} b_j (-\mathrm{i}\omega\Delta t)^j = \mathrm{e}^{-\mathrm{i}\bar{\omega}_2\Delta t}. \tag{8}$$

The target optimization in this case is given by

$$\int_0^{\eta} \left| r_1(\omega\Delta t) r_2(\omega\Delta t) - \mathrm{e}^{-2\mathrm{i}\omega\Delta t} \right|^2 \mathrm{d}\omega\Delta t, \tag{9}$$

while the effective numerical frequency is $\bar{\omega} = (\bar{\omega}_1 + \bar{\omega}_2)/2$, which may be used to calculate the phase error ε_p. Since a p_1-p_2 scheme evaluates $\boldsymbol{F}(\boldsymbol{U})$ $p_1 + p_2$ times to step the time forward by $2\Delta t$, such schemes have the same computational cost as a $(p_1 + p_2)$-stage Runge–Kutta scheme with a time step of $2\Delta t$. Hu et al. [10] proposed a 4-6 and a 5-6 alternating scheme. Figure 3 shows the phase error for these schemes together with the comparable 10- and 11-stage maximal order schemes, while figure 4 compares which is the more accurate for a given value of $\omega\Delta t$. The maximal order schemes are clearly more accurate for the majority of values of $\omega\Delta t$ despite using a twice as long time step as the optimized schemes.

B. Stability limits

Optimization of Runge–Kutta schemes are often restricted by a stability criterion. For real ω, $|r_e(\omega\Delta t)| = \left|\exp\{-\mathrm{i}\omega\Delta t\}\right| = 1$, meaning oscillation with no growth or decay. A given scheme is said to be stable for $0 < \omega\Delta t < \eta_s$ if $|r(\omega\Delta t)| < 1$ for $0 < \omega\Delta t < \eta_s$; that is, the numerical scheme oscillates with possibly decay in amplitude, but with no growth. In general, suppose a p-stage Runge–Kutta scheme is q-th order accurate with $q \geq 1$, so that

$$r(\omega\Delta t) = 1 + \sum_{j=1}^{q} \frac{1}{j!} (-\mathrm{i}\omega\Delta t)^j + \sum_{j=q+1}^{p} c_j (-\mathrm{i}\omega\Delta t)^j. \tag{10}$$

For real ω, in the limit $\Delta t \to 0$, it can be shown that

$$\mathrm{Re}\Big(\log\big(r(\omega\Delta t)\big) \Big) = \begin{cases} (-1)^{n+1} \left[\left(c_{2n+2} - \dfrac{1}{(2n+2)!} \right) - \left(c_{2n+1} - \dfrac{1}{(2n+1)!} \right) \right] (\omega\Delta t)^{2n+2} + O\big((\omega\Delta t)^{2n+4}\big) & \text{if } q = 2n, \\ (-1)^n \left(c_{2n} - \dfrac{1}{(2n)!} \right) (\omega\Delta t)^{2n} + O\big((\omega\Delta t)^{2n+2}\big) & \text{if } q = 2n-1, \end{cases} \tag{11}$$

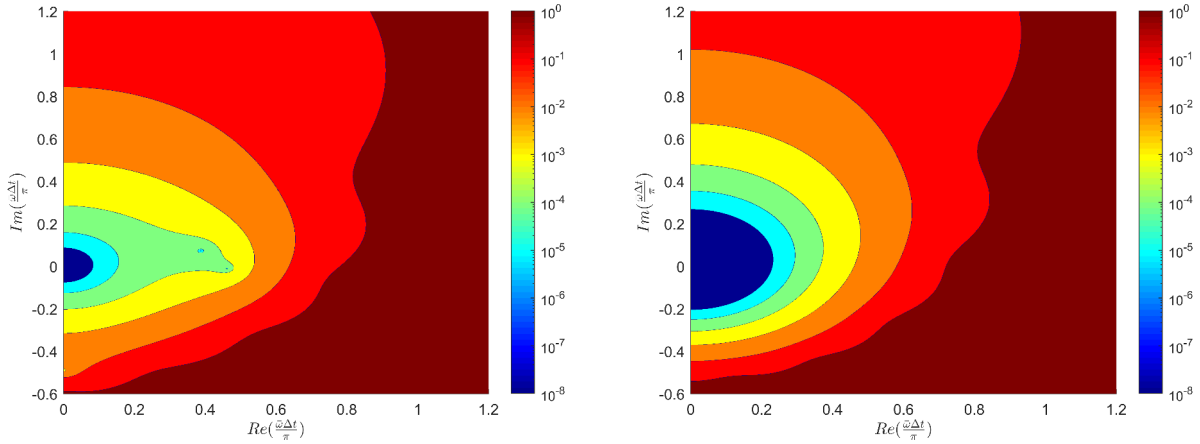

(a) 4th Order LDDRK46(Δt) **(b) Maximal Order RK10(2Δt)**

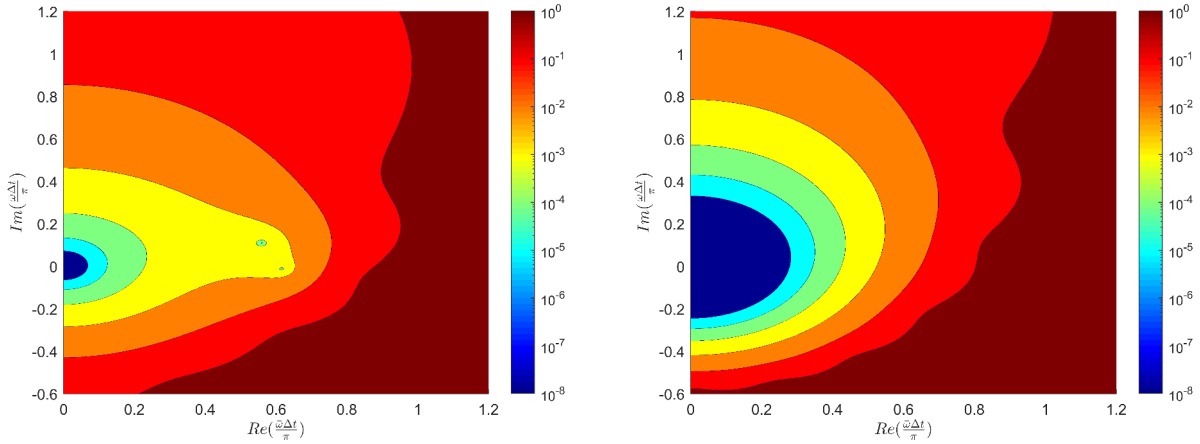

(c) 4th Order LDDRK56(Δt) **(d) Maximal Order RK11(2Δt)**

Fig. 3 Plots of phase error ε_p in the complex $\omega\Delta t$ plane for the LDDRK46 and LDDRK56 schemes of Hu et al. [10], and for maximal order 10-step and 11-step Runge–Kutta schemes with a time step of $2\Delta t$.

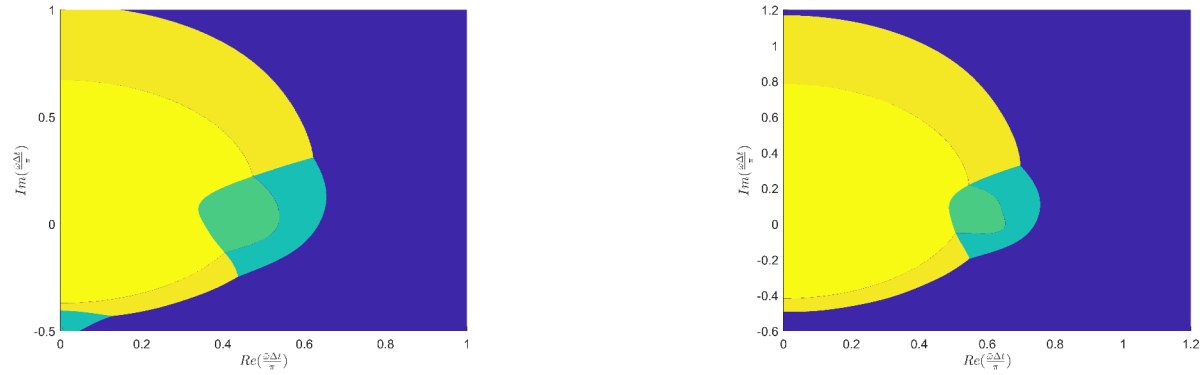

(a) LDDRK46(Δt) vs RK10(2Δt) **(b) LDDRK56(Δt) vs RK11(2Δt)**

Fig. 4 Comparison in the complex $\omega\Delta t$ plane of where the maximal-order (yellow) or LDDRK (green) schemes are more accurate. Darker regions indicate where neither scheme is 0.1% accurate ($\varepsilon_p > 10^{-3}$), while violet regions indicate where neither scheme is 1% accuracy ($\varepsilon_p > 10^{-2}$).

p	3	4	5	6	7	8	9	10	11	12	13	14	15	16
η_s	1.73	2.83	0	0	1.76	3.40	0	0	1.70	3.38	0	0	1.67	3.32
η_{1e-3}	0.39	0.65	0.95	1.26	1.59	1.93	2.27	2.62	2.98	3.34	3.70	4.06	4.42	4.79
η_{1e-4}	0.22	0.41	0.65	0.91	1.19	1.49	1.80	2.13	2.46	2.79	3.14	3.48	3.83	4.18
η_{1e-5}	0.12	0.26	0.44	0.65	0.89	1.15	1.43	1.73	2.03	2.34	2.66	2.98	3.32	3.65
$\hat{\eta}_{1e-3}$	0.36	0.59	0.84	1.10	1.36	1.63	1.91	2.18	2.46	2.74	3.02	3.29	3.57	3.85
$\hat{\eta}_{1e-4}$	0.21	0.39	0.59	0.82	1.06	1.31	1.56	1.82	2.09	2.36	2.63	2.90	3.17	3.44
$\hat{\eta}_{1e-5}$	0.12	0.25	0.41	0.60	0.82	1.04	1.27	1.52	1.77	2.02	2.28	2.54	2.81	3.07

Table 1 Properties of $r(\omega\Delta t)$ for p-stage maximal order Runge–Kutta timestepping schemes.

LDDRK	4	5	6	46	56	BBo5s	BBo6s	$(\mathrm{RK8})^{11/16}$	$(\mathrm{RK12})^{11/24}$
order	2	2	4	4	4	2	2	8	12
stages	4	5	6	5	5.5	5	6	5.5	5.5
η_s	0	1.51	1.66	1.36	2.84	3.56	3.94	2.33	1.55
η_{1e-3}	0.82	1.34	1.75	1.64	2.00	0.98	1.47	1.38	1.62
η_{1e-4}	0.33	0.48	0.75	1.49	0.77	0.41	0.54	1.07	1.36
η_{1e-5}	0.14	0.26	0.46	0.57	0.47	0.19	0.24	0.83	1.14
$\hat{\eta}_{1e-3}$	0.49	0.69	0.92	0.98	0.91	0.79	0.97	1.16	1.32
$\hat{\eta}_{1e-4}$	0.27	0.43	0.63	0.68	0.62	0.39	0.49	0.93	1.14
$\hat{\eta}_{1e-5}$	0.13	0.26	0.42	0.47	0.42	0.19	0.24	0.74	0.98

Table 2 Properties of $r(\omega\Delta t)$ for various optimized timestepping schemes. For the two-stage LDDRK schemes, $r(\omega\Delta t) = \sqrt{r_1(\omega\Delta t) r_2(\omega\Delta t)}$. Maximal Order Runge–Kutta schemes with altered timestep are denoted, e.g. $(\mathrm{RK12})^{11/24}$ for a 12-stage scheme with a timestep $24\Delta t/11$, giving the equivalent $r(\omega\Delta t) = \left(r_{12}(\omega\, 24\Delta t/11)\right)^{11/24}$.

Consequently, in order not to be unstable for arbitrarily small $\omega\Delta t$, we require either $(-1)^{q/2}[(c_{q+1} - 1/(q+1)!) - (c_{q+2} - 1/(q+2)!)] < 0$ if q is even or $(-1)^{(q+1)/2}(c_{q+1} - 1/(q+1)!) < 0$ if q is odd. This is satisfied for all the optimized Runge–Kutta schemes of Bogey and Bailly [7], and all the LDDRK schemes [10] apart from the LDDRK4 scheme, which is therefore (slightly) unstable for arbitrarily small real $\omega\Delta t$. For maximal order schemes, where $q = p$ and there is no flexibility in the choice of coefficients $c_j = 1/j!$, we find that they are stable for some $\eta_s > 0$ if and only if $p = 4m$ or $p = 4m - 1$ for some integer m. In particular, this means that RK4, RK8, RK11, RK12 and RK16 are all stable for some η_s. Stability limits η_s are shown in tables 1 and 2.

It is unclear what the equivalent restriction for complex frequencies should be. One could consider the condition that $|r(\omega\Delta t)/r_e(\omega\Delta t)| < 1$, meaning that the numerical scheme gives a lower growth rate than the exact solution, although this is not necessarily a desirable property to have. It may be that the notion of stability of a timestepping scheme is only relevant to real frequencies, while accuracy is important both for real and complex frequencies.

C. Accuracy limits for real and complex frequencies

By analogy with the real-frequency stability limit η_s above, we may define the real-frequency accuracy limit η_δ such that $\varepsilon_r < \delta$ for $0 < \omega\Delta t < \eta_\delta$. Here, motivated by (7) and a typical lower-bound order of magnitude $T/\Delta t \approx 100$, we will be particularly interested in $\delta = 10^{-4}$ and $\delta = 10^{-5}$, although we will also consider $\delta = 10^{-3}$ since this appears to be the error most optimized schemes have been optimized for. Since we are also interested in the behaviour of timestepping schemes for non-constant-amplitude oscillations, corresponding to complex frequencies ω, we define the analogous complex-frequency accuracy limit $\hat{\eta}_\delta$ such that $\varepsilon_r < \delta$ for $0 < |\omega\Delta t| < \eta_\delta$; that is, an accuracy of $\varepsilon_r < \delta$ is guaranteed irrespective of $\arg(\omega\Delta t)$ provided $|\omega\Delta t| < \eta_\delta$.

These accuracy limits, along with the stability limits, are tabulated in table 1 for maximal order Runge–Kutta schemes, and in table 2 for various optimized Runge–Kutta schemes. For the maximal order schemes in table 1, lower order schemes are usually limited by accuracy, while higher order schemes are progressively more limited by

their stability. Behaviour for complex ω and for real ω are broadly comparable, although restricting to real ω does increase slightly the accuracy range. The situation is markedly different for the optimized schemes in table 2, where the optimized schemes outperform their maximal order equivalents for the real-ω $\delta = 10^{-3}$ case, and underperform their maximal order equivalents when either ω is complex, or when the desired error is $\delta \leq 10^{-4}$. This verifies that the optimized schemes have been optimized solely for real ω and errors of 10^{-3} or larger. The one exception to this is the LDDRK46 scheme, which also performs well (only for real-ω) for $\delta = 10^{-4}$, and this will be seen to translate to better behaviour than any of the other optimized schemes in the next section.

Also plotted in table 2 are the results that would be produced with a higher order maximal order Runge–Kutta scheme with a larger timestep. For example, as previously commented, if a 12-stage maximal order scheme is given a timestep $\widehat{\Delta t} = 24\Delta t/11$, then it has the same computational cost as if it were a 5.5-stage scheme with an unscaled timestep Δt. Table 2 compares the 8-stage and 12-stage maximal order timestepping schemes as if they were 5.5-stage schemes, and shows that they outperform the optimized schemes in all cases but the real-ω $\delta = 10^{-3}$ case; the one exception to this is the previously mentioned LDDRK46 scheme, and even then only in the real-ω $\delta = 10^{-4}$ case.

III. Comparison with a realistic test case

We now investigate how the theoretical behaviour described above translates into performance in practice, by comparing the performance of the various timestepping schemes for the realistic 1D wave propagation problem from Ref. 12. The problem to be solved is

$$\frac{\partial p}{\partial t} + \frac{\partial v}{\partial x} = -k_p(x)p, \qquad \frac{\partial v}{\partial t} + \frac{\partial p}{\partial x} = -k_v(x)v. \tag{12}$$

These equations support wave propagation in both the positive and negative x-directions at a wave speed of 1. Equation (12) is solved on a periodic x-domain [0, 24), with initial conditions $v(x, 0) = p(x, 0)$ and damping $k_p(x) = k_v(x)$ as specified in Ref. 12 consisting of a wave packet with wavelength 1 propagating across a damping region of length 2 and decaying by a factor of e^{-6}. By comparing with the analytic solution $p_a(x, t)$, $v_a(x, t)$, the numerical error is then given by

$$\text{Error} = \frac{\sup_{x\in[0,24)} \left\{ \left|p(x,T) - p_a(x,T)\right|, \left|v(x,T) - v_a(x,T)\right| \right\}}{\sup_{x\in[0,24)} \left\{ \left|p_a(x,T)\right|, \left|v_a(x,T)\right| \right\}} \qquad \text{with } T = 24. \tag{13}$$

Figure 5 compares various timestepping schemes for a "perfect" 15-point 14th order maximal order spatial derivative with 32 points per wavelength (PPW), using a "perfect" spatial filter $F_{16,4}$ at each time step, as described in Ref. 12. A "perfect" time integration would then result in an error of approximately 5×10^{-11} using this scheme, giving a noise floor due to the spatial discretization used. As the timestep Δt, or equivalently the CFL number, is reduced, the error is reduced for each scheme, in general at a rate given by the timestepping scheme's order of accuracy, until this noise floor is reached. For too large Δt the schemes become unstable, generally for CFL numbers in the range 1–4. The higher order schemes show a significantly lower error than the lower-order schemes, with the 2nd order optimized schemes of Bogey and Bailly [7] and Hu et al. [10, LDDRK4 and LDDRK5] performing worse than the 4th order RK4 and optimized LDDRK6, LDDRK46 and LDDRK56 [10] schemes, which themselves perform worse than the higher order maximal order RK8–16 schemes, although of course the latter involve more stages and therefore a higher computational cost. However, figure 6 plots the same error against a measure of the numerical cost of the simulation, and the same trend is apparent. The numerical cost is defined to be

$$\text{Cost} = pw(T/\Delta t)(L/\Delta x), \tag{14}$$

where p is the number of Runge–Kutta stages, w is the half-width of the spatial derivative scheme (so the total width is $2w + 1$), $T = 24$ is the total simulation time, $L = 24$ is the simulation spatial length, and Δt and $\Delta x = 1/\text{PPW}$ are the time step and grid spacing. For a target error of 10^{-3}, almost all efficient schemes need to be run very close to their stability limit, although this could be an artifact of using an unnaturally accurate spatial discretization.

If we are interested in achieving an overall accuracy of 10^{-3} using a more conventional spatial discretization, figure 7 shows the error against timestep for a 7-point 6th order (maximal order) spatial derivative using 24 PPW and a standard 7-point 6th order spatial filter. The noise floor achieved with a "perfect" time integration in this case is approximately 5×10^{-4}, which is the limit of accuracy of the spatial discretization. Figure 8 shows the comparable plot of error

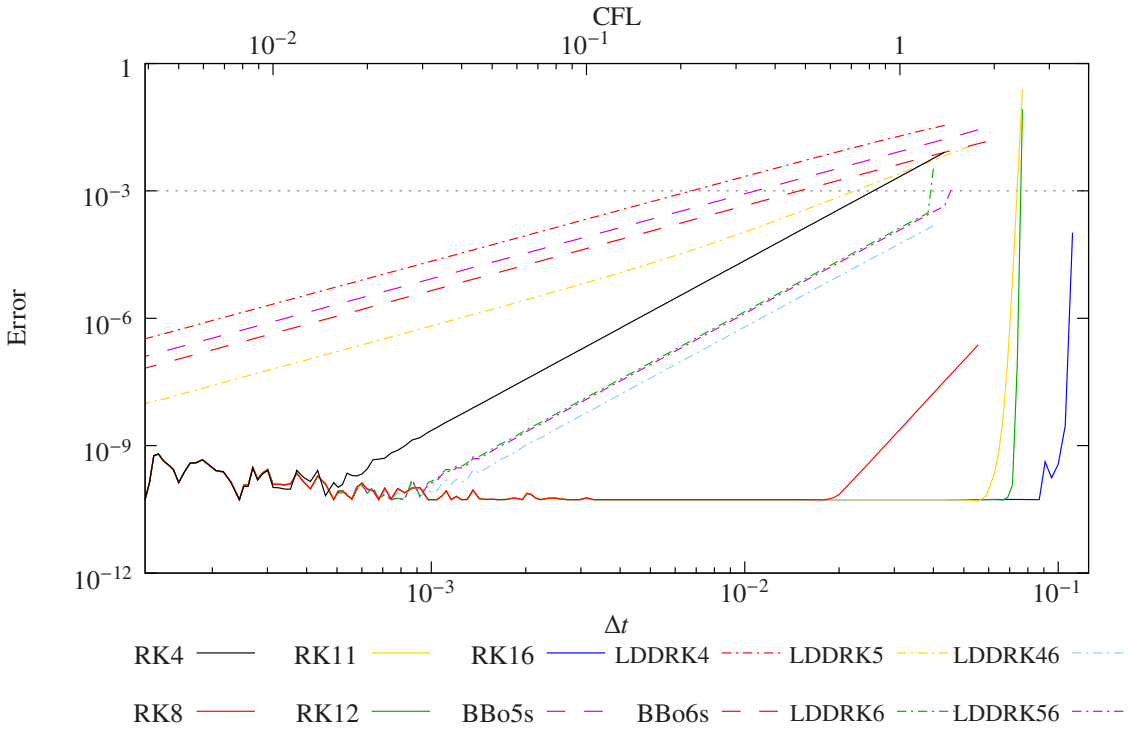

Fig. 5 Error in the numerical solution of (12) **plotted against numerical timestep** Δt **(bottom scale), or equivalently against** CFL = PPWΔt **(top scale), for various timestepping schemes of varying numerical cost. All results are using a "perfect" 15-point 14th order spatial derivative with** PPW = 32 **and the "perfect" 19-point 16th order** $F_{16,4}$ **filter, giving an error of around** 5×10^{-11} **when used with a "perfect" time integration.**

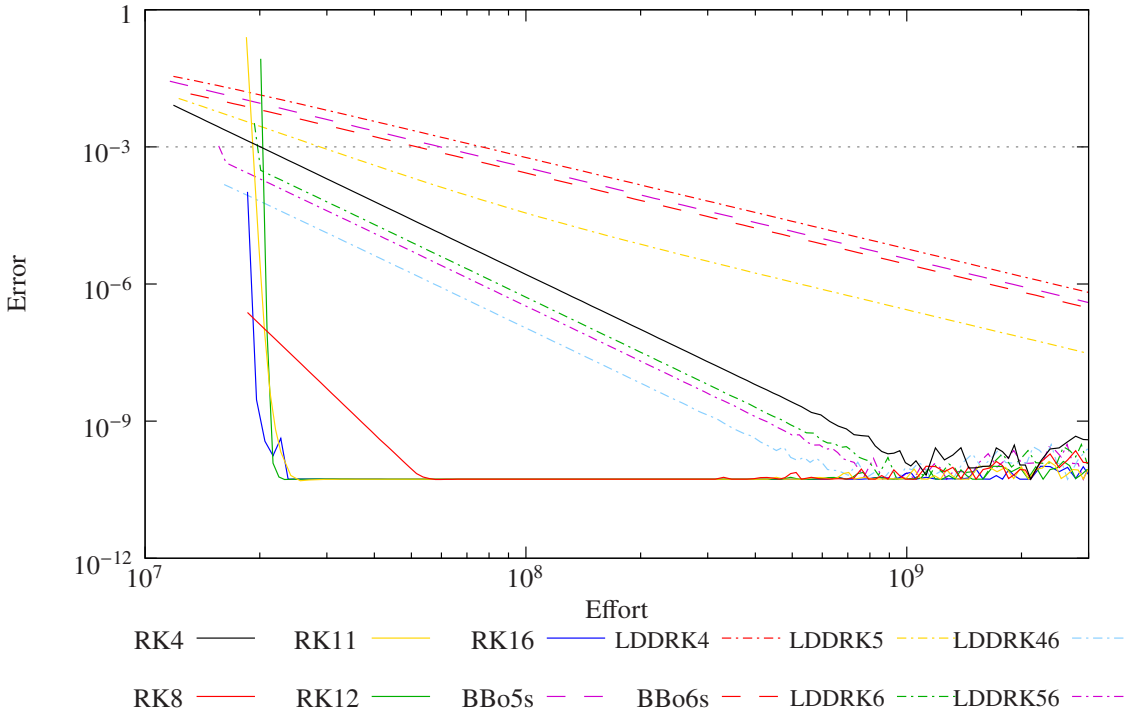

Fig. 6 The equivalent of figure 5 plotting error against the numerical cost (14)**. As for figure 5, a "perfect" 15-point 14th order spatial derivative with** PPW = 32 **and the "perfect" 19-point 16th order** $F_{16,4}$ **filter are used.**

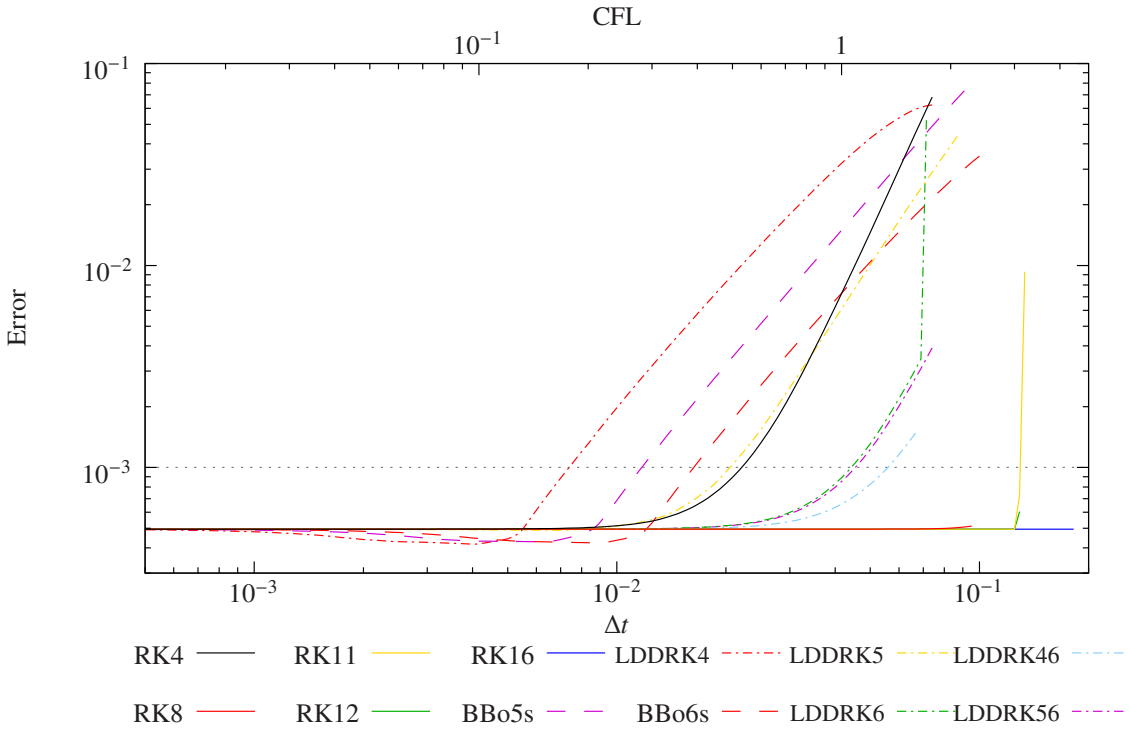

Fig. 7 Error in the numerical solution of (12) **plotted against numerical timestep Δt (bottom scale), or equivalently against CFL (top scale). All results are using a 7-point 6th order spatial derivative with** PPW = 24 **and the 7-point 6th order F_6 filter, giving an error of around 5×10^{-4} when used with a "perfect" time integration.**

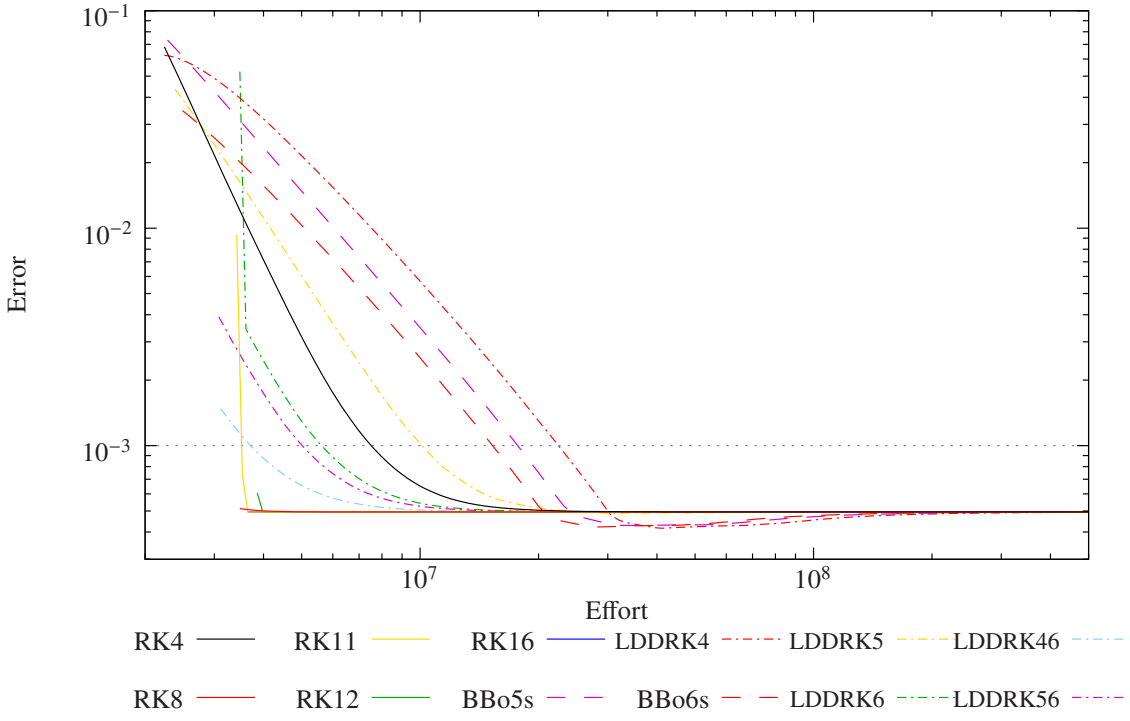

Fig. 8 The equivalent of figure 7 plotting error against the numerical cost (14)**. As for figure 7, a 7-point 6th order spatial derivative with** PPW = 24 **and the 7-point 6th order F_6 filter are used.**

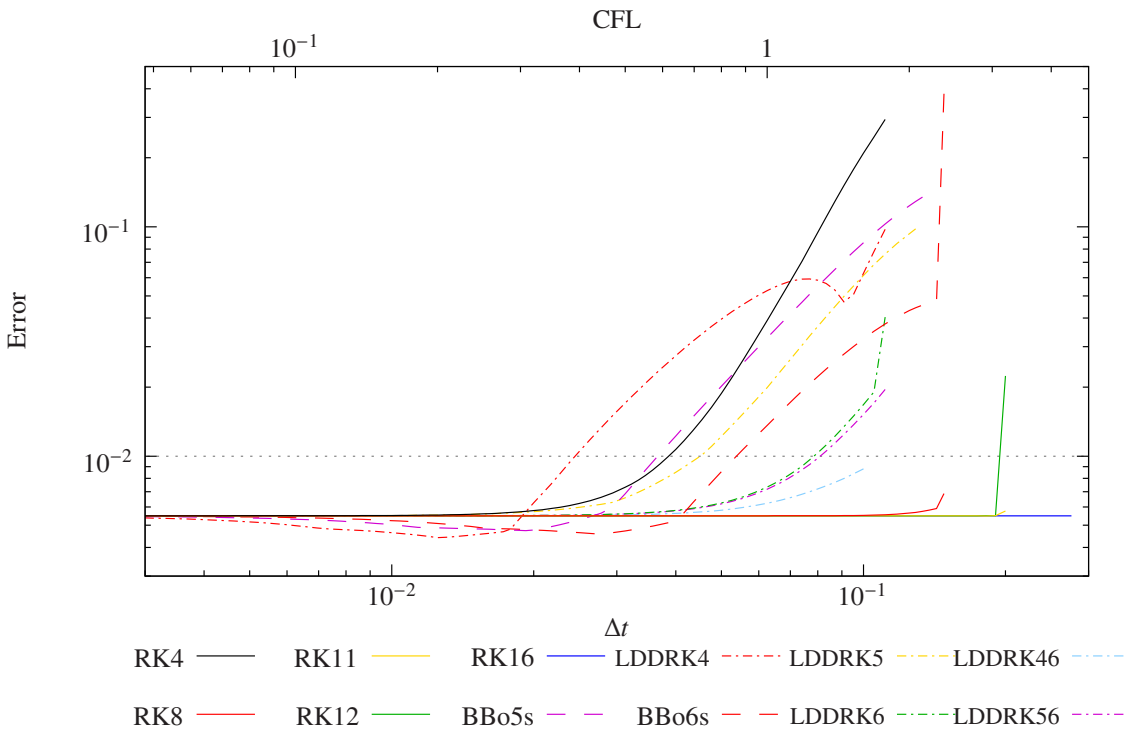

Fig. 9 Error in the numerical solution of (12) **plotted against numerical timestep Δt (bottom scale), or equivalently against CFL (top scale). All results are using a 7-point 6th order spatial derivative with** PPW = 16 **and the 7-point 6th order F_6 filter, giving an error of around 5×10^{-3} when used with a "perfect" time integration.**

against numerical effort. Apart from the worse performance of the RK4 scheme, the same trend as in figures 5 and 6 is apparent. In particular, the commonly used LDDRK56 scheme requires CFL = 1.09 in order to efficiently achieve the desired accuracy, and the higher order maximal order schemes, while potentially 30% more computationally efficient for the same accuracy, require an even higher CFL number to achieve this which is close to their stability limit. The LDDRK46 scheme outperforms the LDDRK56 scheme despite having fewer stages per timestep on average; this is possibly due to the better performance at errors of $\delta = 10^{-4}$ seen in table 2 for this scheme, due to its less aggressive optimization. However, it could be argued that the spatial discretization in this example has significantly more points per wavelength than is usual in practice.

Dropping the required accuracy to 10^{-2} and using 16 points per wavelength results in figure 9, with a "perfect" time integration noise floor of approximately 5×10^{-3}. Figure 10 shows the comparable plot of error against numerical effort. For this situation, the LDDRK5 scheme starts to show some of the expected optimized behaviour of the optimized timestepping schemes, although at errors of around 0.05 which do not benefit the desired accuracy of 0.01. Once again the higher order maximal order schemes give the best accuracy, and once again they must be run near their stability threshold for efficiency. The most computationally efficient scheme to reach an error of 0.01 first is, rather surprisingly, the LDDRK46 scheme, although at an unusually high CFL number of 1.6 at its stability limit.

In practice, optimized spatial derivatives are optimized to work efficiently at around 6 points per wavelength or fewer. In Ref. 12 it was shown that such optimized schemes do not perform well in this test case involving non-constant-amplitude waves. As an example, figure 11 shows the results of using the 7-points 4th order DRP spatial derivative of Tam and Shen [2], together with a standard 7-point 6th order spatial filter. The noise floor achieved with a "perfect" time integration in this case is only 0.2 (i.e. an error of 20%). The optimized timestepping schemes can be seen from figure 11 to also be optimized for this overly ambitious case, with many achieving an error of around 0.3 or lower more quickly than would be expected from a simple power law error decay. Figure 12 shows the comparable error against computational effort plot. It is unclear what error would be being targeted in this case, and although the optimized schemes do seem to outperform the maximal order schemes when comparing error against computational effort in this case, the errors are all sufficiently large that no scheme could be said to have properly converged.

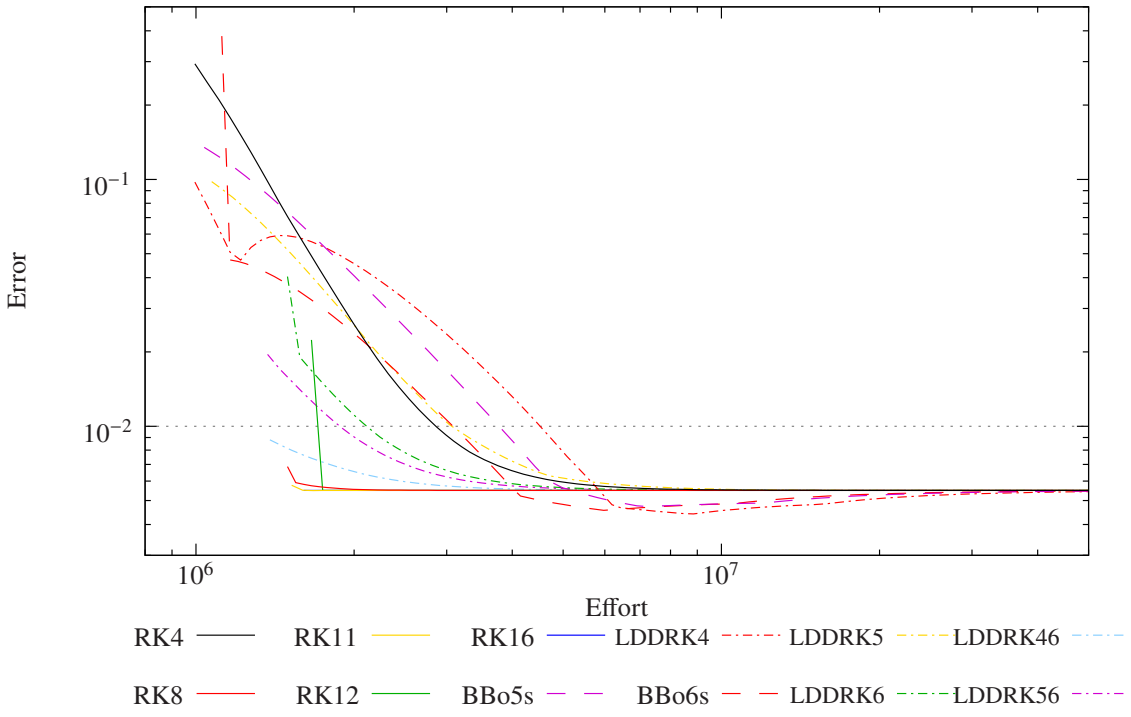

Fig. 10 The equivalent of figure 9 plotting error against the numerical cost (14)**. As for figure 9, a 7-point 6th order spatial derivative with** PPW = 16 **and the 7-point 6th order** F_6 **filter are used.**

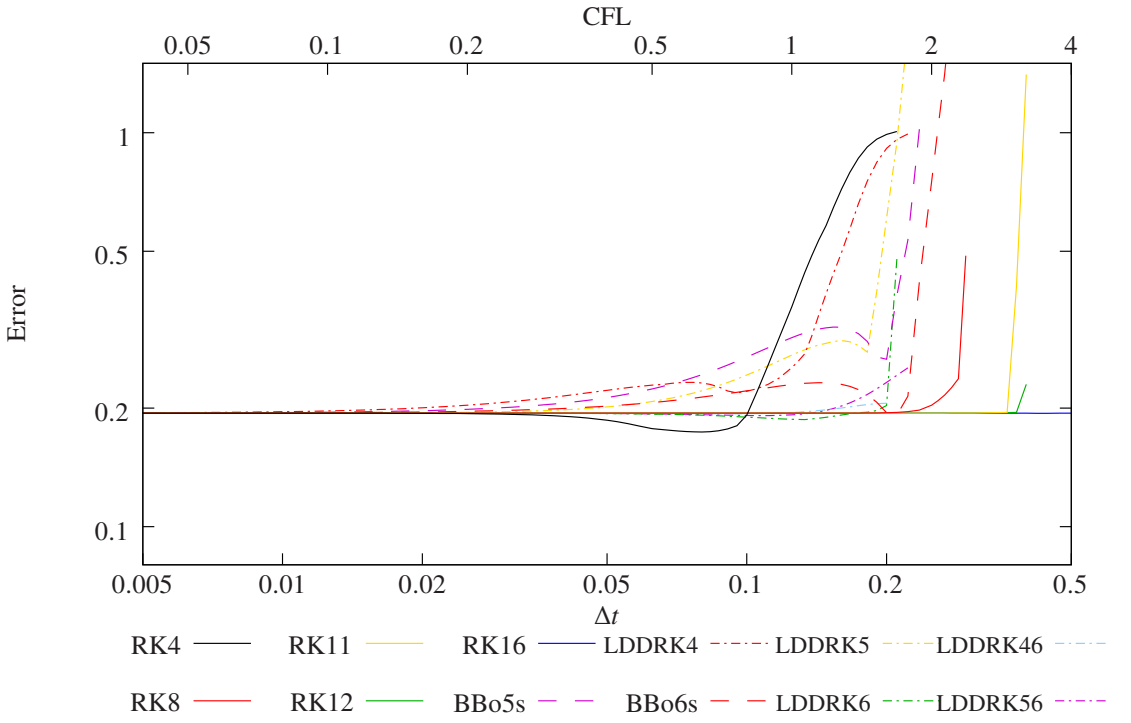

Fig. 11 Error in the numerical solution of (12) **plotted against numerical timestep** Δt **(bottom scale), or equivalently against CFL (top scale). All results are using the 7-point 4th order DRP spatial derivative of Tam and Shen [2] with** PPW = 8 **and the 7-point 6th order** F_6 **filter, giving an error of around** 0.2 **when used with a "perfect" time integration.**

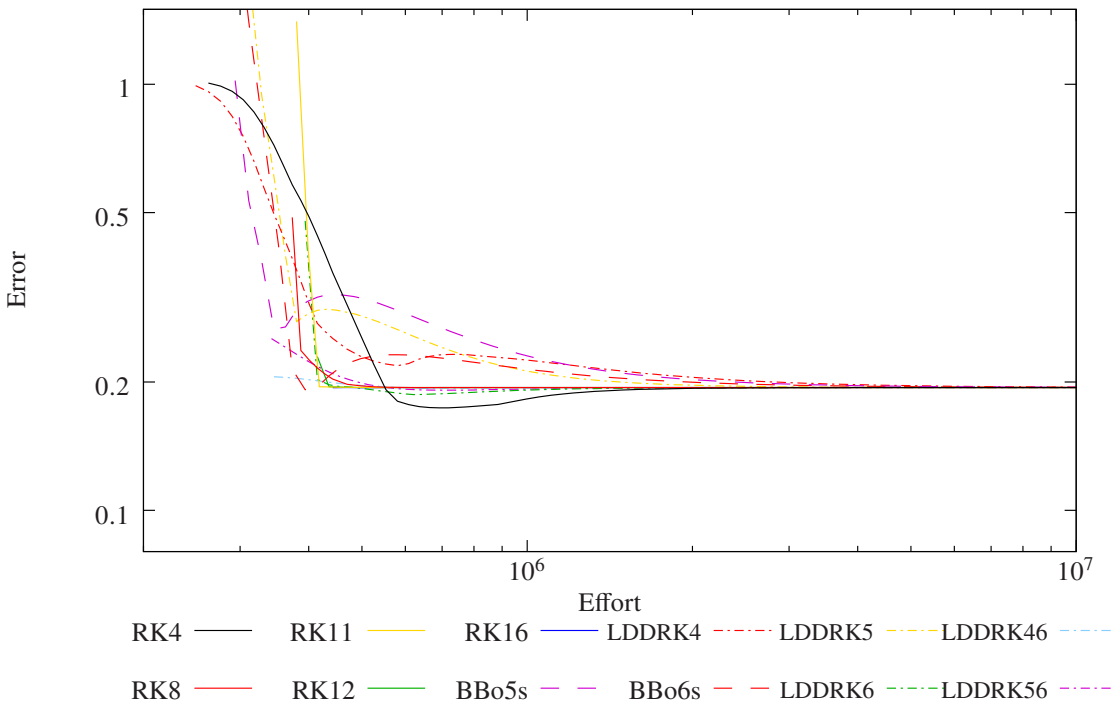

Fig. 12 The equivalent of figure 11 plotting error against the numerical cost (14)**. As for figure 11, the 7-point 4th order DRP spatial derivative of Tam and Shen [2] with** PPW = 8 **and the 7-point 6th order** F_6 **filter are used.**

IV. Conclusion

This paper has investigated Runge–Kutta timestepping schemes optimized to solve acoustics problems. By analogy with optimized spatial derivatives (DRP schemes), which were found to behave poorly for waves of growing or decaying amplitudes [12], it was found here that optimized timestepping schemes have also been optimized assuming real frequencies and hence constant amplitude oscillations, and also perform poorly for waves of growing or decaying amplitude. In particular, figure 4 shows that maximal order schemes are more accurate than optimized LDDRK46 or LDDRK56 schemes [10] for the same computational effort apart from for a rather limited range of nearly-real frequencies; targeting these frequencies would require significant a priori knowledge of the simulation to be performed, and is likely impossible for broadband simulations.

The theory was illustrated by solving an example 1D wave equation in section III taken from Ref. 12. The results suggest that optimized timestepping schemes have been over-ambitiously optimized with target errors of around $\delta = 10^{-3}$ *per timestep*, where as significantly smaller errors are required to get an overall simulation error of around 10^{-2} or 10^{-3}. The results also suggest that the best computational efficiency for a given target accuracy is obtained when the timestepping scheme is very close to its stability limit, with unusually large CFL numbers of 1.5–2 being typically optimal. As was found in Ref. 12, significantly more points per wavelength are needed for the spatial derivatives (around 16 PPW) than are commonly thought necessary to achieve even a modest accuracy of 1% error, and optimized DRP spatial derivatives perform worse than maximal order spatial derivatives.

While the accuracy of timestepping schemes for non-constant-amplitude waves (with complex ω) is a straightforward extension of the notion of accuracy for constant-amplitude waves (with real ω), the same is not true for the stability of timestepping schemes. Indeed, a timestepping scheme is stable for constant-amplitude waves if the numerical solution does not grow in time, meaning only under-predicted growth rates are allowed. It is probably undesirable to require that the amplitude of non-constant-amplitude waves is always under-predicted numerically, and rather growth- and decay-rates of non-constant-amplitude waves are desired to be modelled numerically as accurately as possible. This suggests that the concept of stability for timestepping schemes is restricted to only constant-amplitude waves (with real ω), and no extension to the concept of stability is needed for non-constant-amplitude waves.

Further research is underway to investigate whether timestepping schemes can be optimized for non-constant-amplitude waves, in a similar way to the optimization of spatial derivatives for non-constant-amplitude waves [13].

Acknowledgments

AP gratefully acknowledges funding from the Undergraduate Research Summer Studentship (URSS) scheme at the University of Warwick. EJB gratefully acknowledges funding from a Royal Society University Research Fellowship (UF150695).

References

[1] Tam, C. K. W., and Webb, J. C., "Dispersion-Relation-Preserving Finite Difference Schemes for Computational Acoustics," *J. Comput. Phys.*, Vol. 107, 1993, pp. 262–281. doi:10.1006/jcph.1993.1142.

[2] Tam, C. K. W., and Shen, H., "Direct Computation of Nonlinear Acoustic Pulses using High-Order Finite Difference Schemes," AIAA paper 93-4325, 1993. doi:10.2514/6.1993-4325.

[3] Kim, J. W., and Lee, D. J., "Optimized Compact Finite Difference Schemes with Maximum Resolution," *AIAA J.*, Vol. 34, No. 5, 1996, pp. 887–893. doi:10.2514/3.13164.

[4] Kim, J. W., "Optimised Boundary Compact Finite Difference Schemes for Computational Aeroacoustics," *J. Comput. Phys.*, Vol. 225, 2007, pp. 995–1019. doi:10.1016/j.jcp.2007.01.008.

[5] Hixon, R., and Turkel, E., "Compact Implicit MacCormack-type Schemes with High Accuracy," *J. Comput. Phys.*, Vol. 158, No. 1, 2000, pp. 51–70. doi:10.1006/jcph.1999.6406.

[6] Tang, L., and Baeder, J. D., "Uniformly Accurate Finite Difference Schemes for p-Refinement," *SIAM J. Sci. Comput.*, Vol. 20, No. 3, 1999, pp. 1115–1131. doi:10.1137/S1064827596308354.

[7] Bogey, C., and Bailly, C., "A Family of Low Dispersive and Low Dissipative Explicit Schemes for Flow and Noise Computations," *J. Comput. Phys.*, Vol. 194, 2004, pp. 194–214. doi:10.1016/j.jcp.2003.09.003.

[8] Berland, J., Bogey, C., Marsden, O., and Bailly, C., "High-order, Low Dispersive and Low Dissipative Explicit Schemes for Multiple-scale and Boundary Problems," *J. Comput. Phys.*, Vol. 224, 2007, pp. 637–662. doi:10.1016/j.jcp.2006.10.017.

[9] Turner, J. M., Haeri, S., and Kim, J. W., "Improving the Boundary Efficiency of a Compact Finite Difference Scheme through Optimising its Composite Template," *Computers & Fluids*, Vol. 138, 2016, pp. 9–25. doi:10.1016/j.compfluid.2016.08.007.

[10] Hu, F. Q., Hussaini, M. Y., and Manthey, J. L., "Low-Dissipation and Low-Dispersion Runge–Kutta Schemes for Computational Acoustics," *J. Comput. Phys.*, Vol. 124, 1996, pp. 177–191. doi:10.1006/jcph.1996.0052.

[11] Rona, A., Spisso, I., Hall, E., Bernardini, M., and Pirozzoli, S., "Optimised Prefactored Compact Schemes for Linear Wave Propagation Phenomena," *J. Comput. Phys.*, Vol. 328, 2017, pp. 66–85. doi:10.1016/j.jcp.2016.10.014.

[12] Brambley, E. J., "Optimized finite-difference (DRP) schemes perform poorly for decaying or growing oscillations," *J. Comput. Phys.*, Vol. 324, 2016, pp. 258–274. doi:10.1016/j.jcp.2016.08.003.

[13] Brambley, E. J., and Markevičiūtė, V. K., "Optimization of DRP schemes for non-constant-amplitude oscillations," AIAA paper 2017-3175, 2017. doi:10.2514/6.2017-3175.